Supporting Information

Suppressed Efficiency Roll-off in Blue Light-Emitting Diodes by Balancing the Spatial Charge Distribution

Fangfang Wang,[a,b] Huimin Zhang,[a,b] Qingli Lin,[b,*] Jiaojiao Song,[b] Huaibin Shen,[b] Hanzhuang Zhang,[a,*] Wenyu Ji[a,*]

[†]Key Lab of Physics and Technology for Advanced Batteries (Ministry of Education), College of Physics, Jilin University, Changchun 130012, China

[‡]Key Laboratory for Special Functional Materials of Ministry of Education, Henan University, Kaifeng 475004, China

Preparation of the FTIR samples

The samples were prepared on silicon wafers with the scale of ~2 cm × 2 cm. Before to use, the silicon wafers were put into detergent, ultrapure water, acetone and isopropanol for ultrasonic cleaning for 15 min.

Sample before ligand exchange: ZnCdSeS QD solution (18 mg/mL, octane) was spin-coated onto the silicon wafer at 3000 rpm for 30 s.

Sample after ligand exchange: The obtained QD film was soaked with the propanethiol/acetonitrile solution for 30 s (the volume ratio of propanethiol to acetonitrile is 1:10), where the propanethiol/acetonitrile solution is required to cover the entire film. After that, the solution was spun off at 3000 rpm for 1 min. Then, acetonitrile is cast onto the QD film and spin-casting at 3000 rpm to wash away the exchanged ligands as well as the excess of new short ligands, and this process is repeated three times.

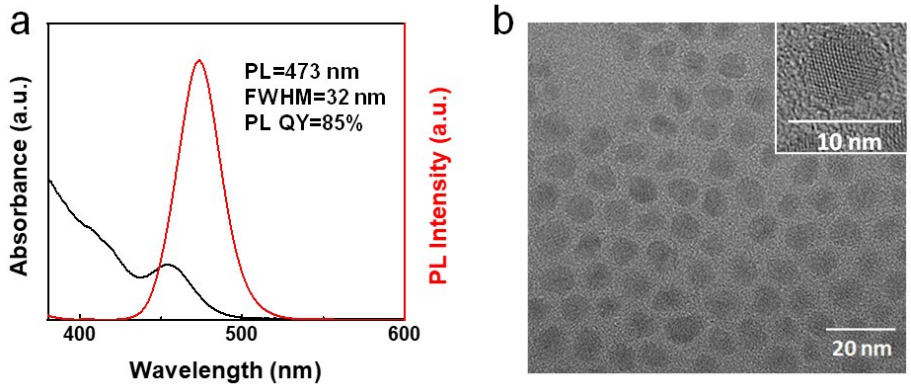

Figure S1. (a) UV-vis and PL spectra of ZnCdSeS QDs. (b)TEM image of ZnCdSeS QDs, the inset is HRTEM.

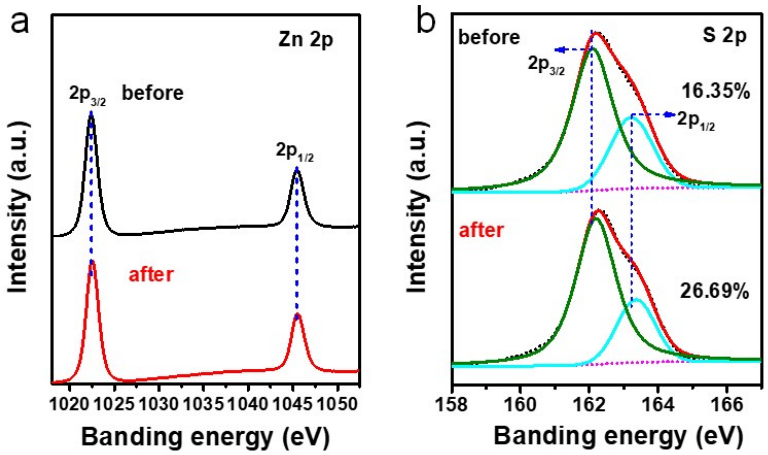

Figure S2. XPS spectra of (a) Zn 2p and (b) S 2p before and after ligand exchange.

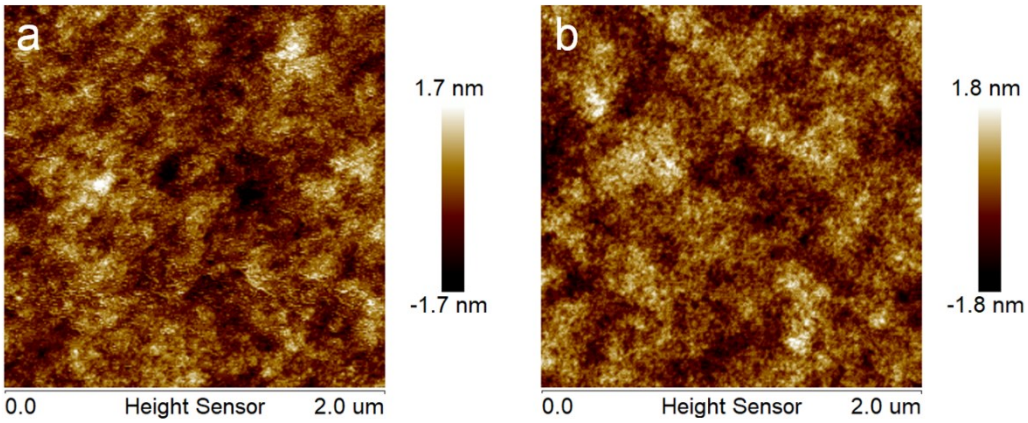

Figure S3. AFM images of TFB hole transport layer before (left) and after (right) treatment by propanethiol solution (dissolved in acetonitrile). The root mean squared roughness (R_q) is 0.486 and 0.513 nm, respectively.

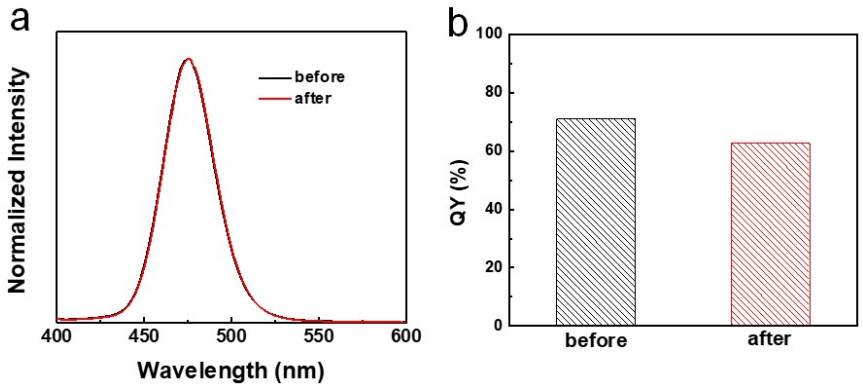

Figure S4. (a) Normalized PL spectra and (b) PL QY of ZnCdSeS QD films before and after propanethiol ligand exchange.

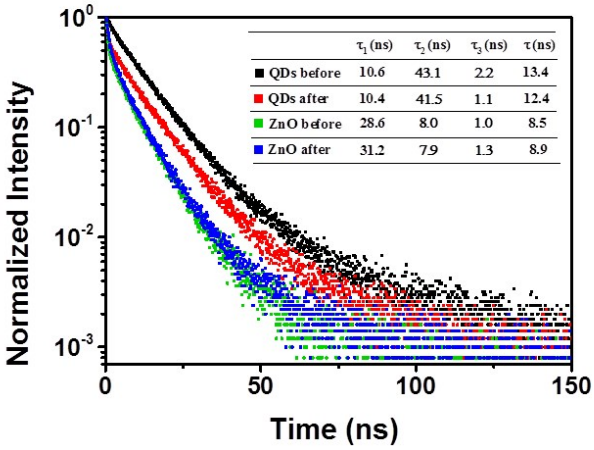

Figure S5. PL lifetime of ZnCdSeS QD films before and after propanethiol ligand exchange, and the corresponding PL lifetime of QDs contacting ZnO layers.

Table S1. PL Lifetime of ZnCdSeS and ZnCdSeS/ZnO QD films before and after ligand exchange. The PL decay curves were fitted to a tri-exponential function to investigate the exciton dynamics of these QD films. The intensity-weighted average exciton lifetime (τ_{avr}) was $B_1\tau_1 + B_2\tau_2 + B_3\tau_3$, where B_1, B_2 and B_3 are fractional intensities and τ_1, τ_2 and τ_3 are lifetimes.

film	τ_1(ns)	τ_2(ns)	τ_3(ns)	B_1(%)	B_2(%)	B_3(%)	τ(ns)	χ^2
ZnCdSeS (before)	10.6	43.1	2.2	84.0	10.1	5.9	13.4	1.098
ZnCdSeS (after)	10.4	41.5	1.1	85.0	8.4	6.6	12.4	1.027
ZnCdSeS(before)/ ZnO	28.6	8.0	1.0	7.0	79.7	13.3	8.5	1.005
ZnCdSeS(after)/ZnO	31.2	7.9	1.3	8.3	77.2	14.5	8.9	1.007

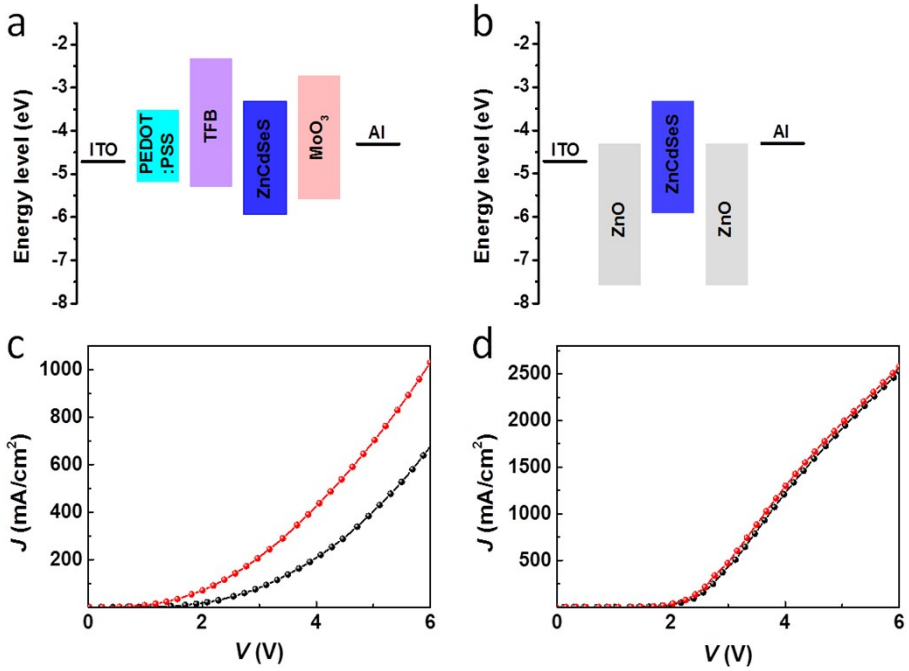

Figure S6. Schematic illustration of energy level of hole-only (a) and electron-only (b) devices. The hole-only device was fabricated as ITO/PEDOT:PSS (60 nm)/TFB (34 nm)/QDs (35 nm)/MoO_3 (8 nm)/Al (100 nm), in which the electrons are blocked by the TFB layer and thus the hole transport behavior can be reflected by the measured current. The structure for the electron-only device is ITO/ZnO (25 nm)/QDs (35 nm)/ZnO (25 nm)/Al (100 nm), where the two ZnO nanoparticle layers on either side of the QDs layer can block the injection of the holes from the electrodes. Current density-voltage curves of (c) hole-only and (d) electron-only devices based on OA- and propanethiol-modified ZnCdSeS QDs.

Comparision of the hole mobility of QDs with propanethiol and OA ligands:

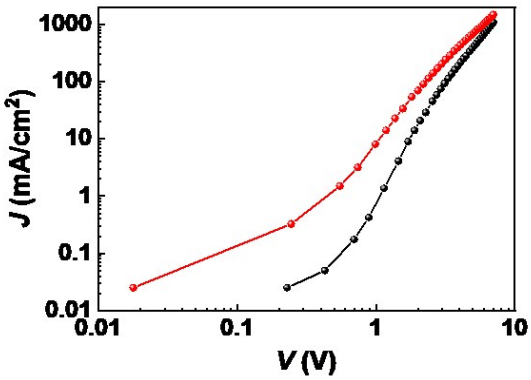

Log-log scale plot of Figure S6c.

By fitting the J-V characteristics in the SCLC region according to the Mott-Gurney Law, $J = ((9\varepsilon\varepsilon_0\mu V^2)/(8t^3))$, where ε_0 is the vacuum permittivity, ε is the relative permittivity of the ZnCdSeS QDs and t = 35 nm is the layer thickness. Correspondingly, J is 84.01 and 240.52 mA/cm^2 before and after exchange, respectively, and V is 2.556 and 2.987 V before and after exchange, respectively. Therefore, we obtain the hole mobility of QDs with propanethiol is 2.1 times higher than that of QDs with OA ligands.

Table S2. Comparison of the maximum luminance of the as-fabricated QLEDs and other QLEDs and OLEDs.

LED Types	Year	PL peak (nm)	L_{max} (cd m^{-2})	*Ref.*
TADF OLED	2007		~50,000(blue)	40
AIE OLED	2009		92,810(Sky-blue)	S1
QLED	2013	452	2624	18
	2014	445	4100	S2
	2015	455	4000	S3(our group)
	2015	441	7600	20
	2017	445	4500	S4 (our group)
	2017	466	4890	11
	2018	445	6768	12 (our group)
	2018	457	10824	S5
	2018	462	16655	S6
	2018	454	20900	S7
	2019	449	7992.5	S8
	2019	474	26800	S9
	2019	452	27753	S10
	2019	464	34874	S11
	2019	465	36970	S12
	2019	476	62600	10 (our group)
	2020	473	52360	This work

Table S3. Comparison of the peak EQE (*max.* η_{EQE}), EQE at 1000 and 10000 cd/m^2, luminance at peak EQE (*L@ max.* η_{EQE}), the critical luminance (L_0) the current density at the peak EQE (*J@ max.* η_{EQE}) and the critical current density (J_0) of the as-fabricated devices and other QLEDs.

Year	η_{EQE} (%)			*L@max.* η_{EQE} (cd/m^2)	L_0 (cd/m^2)	*J@max.* η_{EQE} (mA/cm^2)	J_0 (mA/cm^2)	*Ref.*
	peak	@1000 cd/m^2	@10000 cd/m^2					
2015	10.9	10.7	Null	940	Null	Null	Null	S3
2016	8.76	8.74	Null	1640	Null	Null	Null	S13
2017	19.8	~10	Null	~300	Null	5.53	Null	11
2018	16.2	Null	Null	660	Null	5.6	Null	S7
2019	8.05	6.1	8.04	10100	Null	105	Null	10
2020	9.9	9.7	7.4	1040	28260	9.0	540	This work

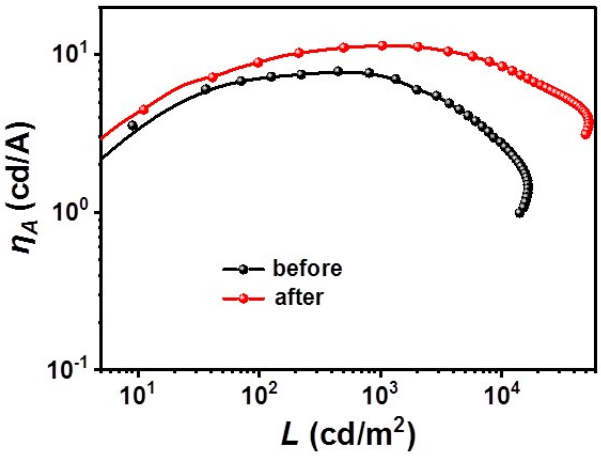

Figure S7. Current efficiency (η_A) as a function of luminance (L) of devices based on ZnCdSeS QDs before and after propanethiol ligand exchange.

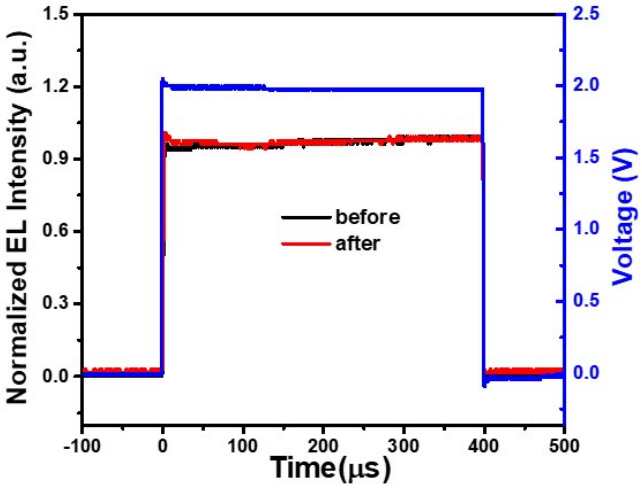

Figure S8. Transient EL (TrEL) response of QLEDs driven by a 4 V voltage pulse with a repetition frequency of 1 kHz (400 μs duty cycle).

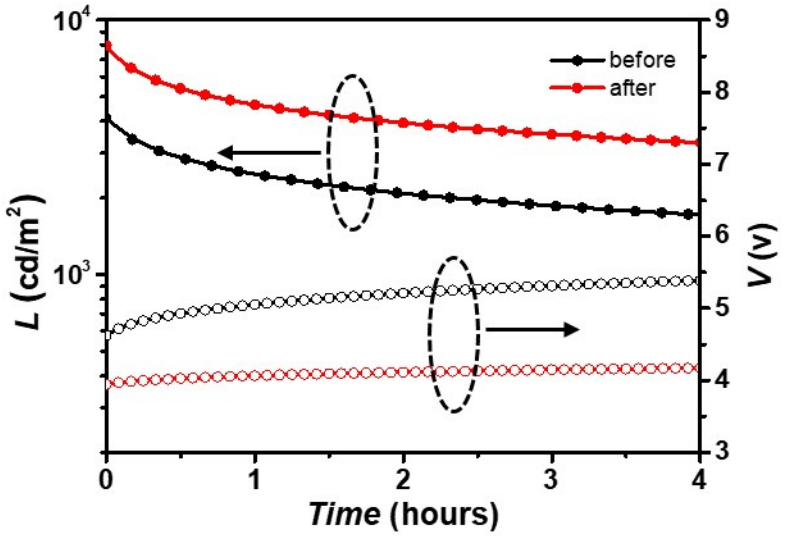

Figure S9. Stability data for a device based on ZnCdSeS QDs. The device was test at ambient conditions (temperature, 20–25℃; relative humidity, 50–70%).

Reference

(S1) Chen, L.; Lin, G.; Peng, H.; Ding, S.; Luo, W.; Hu, R.; Chen, S.; Huang, F.; Qin, A.; Zhao, Z.; Tang, B. Z. Sky-Blue Nondoped OLEDs Based on New AIEgens: Ultrahigh Brightness, Remarkable Efficiency and Low Efficiency Roll-Off. *Mater. Chem. Front.* **2017**, *1*, 176-180.

(S2) Shen, H.; Bai, X.; Wang, A.; Wang, H.; Qian, L.; Yang, Y.; Titov, A.; Hyvonen, J.; Zheng, Y.; Li, L. S. High-Efficient Deep-Blue Light-Emitting Diodes by Using High Quality $Zn_xCd_{1-x}S$/ZnS Core/Shell Quantum Dots, *Adv. Funct. Mater.* **2014**, *24*, 2367-2373.

(S3) Yang, Y.; Zheng, Y.; Cao, W.; Titov, A.; Hyvonen, J.; Manders, J. R.; Xue, J.; Holloway, P. H.; Qain, L. High-Efficiency Light-Emitting Devices Based on Quantum Dots with Tailored Nanostructures, *Nat. Photonics* **2015**, *9*, 259-266.

(S4) Shen, H.; Lin, Q.; Cao, W.; Yang, C.; Shewmon, N. T.; Wang, H.; Niu, J.; Li, L. S.; Xue, J. Efficient and Long-Lifetime Full-Color Light-Emitting Diodes Using High Luminescence Quantum Yield Thick-Shell Quantum Dots, *Nanoscale* **2017**, *9*, 13583-13591.

(S5) Li, J.; Liang, Z.; Su, Q.; Jin, H.; Wang, K.; Xu, G.; Xu, X. Small Molecule-Modified Hole Transport Layer Targeting Low Turn-On-Voltage, Bright, and Efficient Full-Color Quantum Dot Light Emitting Diodes. *ACS Appl. Mater. Interfaces* **2018**, *10*, 3865-3873.

(S6) Wang, F.; Jin, S.; Sun, W.; Lin, J.; You, B.; Li, Y.; Zhang, B.; Hayat, T.; Alsaedi, A.; Tan, Z. Enhancing the Performance of Blue Quantum Dots Light-Emitting Diodes

through Interface Engineering with Deoxyribonucleic Acid. *Adv. Opt. Mater.* **2018**, *6*, 1800578.

(S7) Lin, Q.; Wang, L.; Li, Z.; Shen, H.; Guo, L.; Kuang, Y.; Wang, H.; Li, L. S. Nonblinking Quantum-Dot-Based Blue Light-Emitting Diodes with High Efficiency and a Balanced Charge-Injection Process. *ACS Photonics* **2018**, *5*, 939-946.

(S8) Li, D.; Bai, J.; Zhang, T.; Chang, C.; Jin, X.; Huang, Z.; Xu, B.; Li, Q. Blue Quantum Dot Light-Emitting Diodes with High Luminance by Improving the Charge Transfer Balance. *Chem. Commun.* **2019**, *55*, 3501-3504.

(S9) Zhang, H.; Chen, S.; Sun, X. W. Efficient Red/Green/Blue Tandem Quantum-Dot Light-Emitting Diodes with External Quantum Efficiency Exceeding 21%. *ACS Nano* **2017**, *12*, 697-704.

(S10) Cheng, T.; Wang, F.; Sun, W.; Wang, Z.; Zhang, J.; You, B.; Li, Y.; Hayat, T.; Alsaed, A.; Tan, Z. High-Performance Blue Quantum Dot Light-Emitting Diodes with Balanced Charge Injection. *Adv. Electron. Mater.* **2019**, *5*, 1800794.

(S11) Wang, F.; Sun, W.; Liu, P.; Wang, Z.; Zhang, J.; Wei, J.; Li, Y.; Hayat, T.; Alsaedi, A.; Tan, Z. Achieving Bbalanced Charge Injection of Blue Quantum Dots Light-Emitting Diodes through Transport Layer Doping Strategies. *J. Phys. Chem. Lett.* **2019**, *10*, 960-965.

(S12) Qu, X.; Zhang, N.; Cai, R.; Kang, B.; Chen, S.; Xu, B.; Wang, K.; Sun, X. W. Improving Blue Quantum Dot Light-Emitting Diodes by a Lithium Fluoride Interfacial Layer. *ACS Appl. Phys. Lett.* **2019**, *114*, 071101.

(S13) Wang, L.; Chen, T.; Lin, Q.; Shen, H.; Wang, A.; Wang, H.; Li, C.; Li, L. S. High-Performance Azure Blue Quantum Dot Light-Emitting Diodes via Doping PVK in Emitting Layer. *Org. Electron.* **2016**, 37, 280-286.